Rare Metal Materials and Engineering
Volume 52, Issue 2, February 2023
Available online at www.rmme.ac.cn

Science Press

Cite this article as: Zheng Wei, Wang Yao, He Siliang, et al. Effect of Substrate Type on Morphology of Silica Aerogel Film Prepared by Ambient Pressure Dry Method[J]. Rare Metal Materials and Engineering, 2023, 52(02): 493-501.

ARTICLE

Effect of Substrate Type on Morphology of Silica Aerogel Film Prepared by Ambient Pressure Dry Method

Zheng Wei[1], Wang Yao[1], He Siliang[2], Xiang Xun[1], Cui Yinhua[1], Hu Chuan[1]

[1] Institute of Semiconductors, Guangdong Academy of Sciences, Guangzhou 510650, China; [2] School of Mechanical and Electrical Engineering, Guilin University of Electronic Technology, Guilin 541004, China

Abstract: Silica aerogel films were fabricated on five substrates, i.e., Ti, SiO_2, GaN, Al and Si, by ambient pressure dry method. The influence of the substrate type on the morphology of the silica aerogel films was investigated. X-ray photoelectron spectroscopy (XPS) was used to observe the interfacial bonding states between silica aerogel films and the substrates. The refractive index of each film was measured by fitting the reflectance spectrum using spectroscopic ellipsometry. The morphology and cross-section of each film were observed by atomic force microscope and field emission scanning electron microscope. Results show that the binding energy offset of 0.07 eV of the Al-O center peak and 0.43 eV of the Ti $2p_{3/2}$ center peak are caused by the fabrication of the silica aerogel films, which suggests the formation of chemical bonds between the substrates and the silica aerogel films. The silica aerogel film prepared on the Ti substrate has the lowest refractive index of the films (1.17), and an approximate average porosity of 63.8% which is higher than that of the film on the Si substrate (57.2%). Effect of substrate type on the morphology of silica aerogel film is attributed to hydrophilicity. Owing to the best hydrophilicity of Ti substrate, more particles are accumulated on the Ti substrate to nucleate and grow, producing a silica aerogel film with larger surface roughness, particles and pores than other films.

Key words: silica aerogel film; substrate type; hydrophilicity; molecular polarity; particle nucleation and growth

Highly porous silica aerogel films are considered promising candidates for many applications, including ultra-low-density temperature-resistant insulation materials[1–3], highly efficient high-energy electrodes[4], acoustic impedance coupling materials[5–7], gas adsorption and separation membranes[8–9], and highly efficient catalysts and their carriers[10–11]. Silica aerogel materials have ultra-low thermal conductivity (as low as 0.012 $W \cdot m^{-1} \cdot K^{-1}$ at 25 °C) owing to their skeletal structures and high gas conductance[12]. Their high porosities and large surface areas make them good catalyst carriers and templates for gas sensors. The average pore size of silica aerogel is 10–100 nm, which is close to the mean free path of air molecules. Therefore, silica aerogels are effective sound barriers. They also have low dielectric constants and are adaptable. Furthermore, silica aerogels are resistant to high temperatures: they can withstand temperatures above 500 ° C without structural collapse[13–14]. Moreover, it is possible to tailor their nano-porous structures by controlling their preparation, i. e., the sol-gel process and the drying method.

Silica films can be fabricated by many methods, such as vacuum evaporation[15–17], spin coating a silica sol[18–21], and sol-gel formation from a stagnant solution[22–26]. These methods are implemented on various substrates. However, owing to the difference between chemical structures, it is difficult to form a connection between metals and ceramics. This results in poor adherence between the silica layer and some metals, such as gold (Au) and silver (Ag). Researchers have mostly focused on the surface modification of the metal substrate. To improve the insulating quality of the substrate, it is possible to form an oxide layer on the surface of the metal by electrochemical means to enable molecular adhesion between the silica layer and the metal surface. This method is also used to improve the chemical affinity between silica coatings and metal electrodes. Other researchers have attempted to produce an intermediate

Received date: May 20, 2022
Foundation item: Key-Area Research and Development Program of Guangdong Province (2020B0101320001); Project of Special Fund for Action to Build the First-Class Domestic Research Institution of Guangdong Academy of Sciences (2021GDASYL-20210103080, 2021GDASYL-20210103078); Science and Technology Program Project of Guangzhou (202102020404)
Corresponding author: Zheng Wei, Ph. D., Institute of Semiconductors, Guangdong Academy of Sciences, Guangzhou 510650, P. R. China, E-mail: zhengwei@gdisit.com

layer between the silica coating and the substrate to improve adhesion. The intermediate layer acts as a buffer that can form chemical bonds between the silica film and the substrate through the chemical groups on surface[27–30]. For example, Thompson and Pemberton[31] used (3-mercaptopropyl) trimethoxysilane to facilitate the adhesion of a silica layer to Au or Ag surfaces. Rai and Perry[32] fabricated a polymer film on an Au substrate by forming strong covalent bonds between the Au and silica film that involved hydroxyl groups.

Like adhesion between the film and the substrate, the substrate can affect the morphology of the film[33–35], especially the silica aerogel film. In our opinion, the fabrication of silica aerogel film is not only a hydrolysis-condensation reaction, but also involves the nucleation and growth of particles. The process is affected by many factors, including the stoichiometry, the type and amount of the catalyst, the aging time, and the drying method. Different substrates have different surface chemistries, which can affect the condensation of silica aerogel films. Researchers have investigated the influence of the substrate type on the morphology of the film. Predoana et al[36] prepared indium tin oxide (ITO) films by dip coating using a sol-gel solution. Three substrates were used in the experiment: glass, SiO_2/glass, and Si. A film with a porous structure similar to that of a silica aerogel film was obtained on each substrate. According to the atomic force microscopy (AFM) images, the ITO film deposited on the Si substrate was relatively smooth, whereas that on the SiO_2/glass was rougher. The film deposited on glass had a surface roughness close to that on SiO_2/glass, but the two films differed in thickness. The roughness of the ITO film on the Si substrate increased linearly with the number of depositions. However, the roughness of films on SiO_2/glass and glass substrates was three times larger than that on the Si substrate. Sun et al[37] compared the morphologies of silica aerogel films on Si and SiO_2 buffer substrates, and confirmed that a better interface was achieved on the SiO_2 buffer substrate. The silica aerogel film on the SiO_2 buffer substrate had relatively small pores and greater continuity, whereas the film on the Si substrate contained no uniformly distributed pores or cavities with fixed shapes. Therefore, it was concluded that the hydrophilic SiO_2 buffer substrate can inhibit local shrinkage during gelation and promote the isotropic reaction of the solution after film deposition, which produces uniformly located and well-shaped pores. Jung et al[38] investigated the interface between SiO_2 aerogel film and metal substrate. They found that aluminum silicate bonds formed at the interface during the aging of the spun-on film, and the number of oxidized Al bonds increased after supercritical drying. $Cu(OH)_2$ was generated during the film fabrication process, and copper silicate bonds were formed at the interface of the aged film.

In the present work, the evolution of the morphology of silica aerogel films during spin coating was studied. Five substrates were used including Al, Ti, SiO_2, GaN, and Si. The accumulation of particles and the pore size distribution in silica aerogel films were investigated. The extent of adhesion between the silica aerogel film and each substrate was determined. The effect of the hydrophilicity of each substrate on the morphology of the silica aerogel film was investigated to determine the influence of the characteristics of the substrate surface.

1 Experiment

1.1 Film preparation

Tetraethoxysilane (TEOS, analytical reagent (AR) grade) with a solute concentration of 96% (i.e., the silica source) and hexamethyldisilazane (HMDS; AR 98%; i.e., the hydrophobic agent) were purchased from the China Pharmaceutical Group Co., Ltd. Hydrochloric acid (HCl; AR 36.5%; i. e., the hydrolysis catalyst), aqueous ammonia (NH_4OH; AR 28%; i.e., the condensation catalyst), and n-hexane (AR 99.5%; i.e., the cleaning agent) were provided by Shanghai Aladdin Biochemical Technology Co., Ltd. Ethanol (AR 99.7%; i. e., the sol solvent), acetone (AR 99.5%), and hydrofluoric acid (HF; AR 40%; i.e., the cleaning agent) were purchased from Jiangyin Chemical Reagent Factory Co., Ltd.

TEOS, ethanol, pure water, and HCl were mixed in a molar ratio of 1∶4∶4∶2 ($\times10^{-3}$) to form a silica aerosol. The aerosol was immediately transferred to a water bath and stirred at 60 °C for 2 h. As a result, TEOS was hydrolyzed completely. Five types of substrates were used in the experiment to determine their effect on the fabrication of the silica aerogel film. Si substrate (500 μm in thickness) and SiO_2 substrate (500 nm in thickness) whose surface was formed by thermal oxidation were purchased from the Shenzhen Rigorous Technology Co., Ltd. Al coating (500 nm in thickness) was deposited on the Si substrate by electron beam evaporation at 30 °C under 2.6×10^{-4} Pa at a deposition rate of 0.14 nm/s to obtain the Al substrate. Similarly, Cu coating (480 nm in thickness) was deposited on the Si substrate at 30 °C under 2.6×10^{-4} Pa at a deposition rate of 0.15 nm/s. Owing to the high activity of elemental Cu, the copper atoms readily escape from the Si substrate in such an arrangement, resulting in flaking of the Cu coating. Therefore, in the present study, a protective Ti coating (10 nm in thickness) was deposited on the surface of the Cu coating at 30 °C under 2.6×10^{-4} Pa at a deposition rate of 0.05 nm/s. Ti substrate was thereby obtained. GaN substrate with 5 μm in thickness was offered by Institute of Semiconductors, Guangdong Academy of Sciences, which was prepared by the method mentioned in Ref. [39].

The Si substrate was pretreated with HF solution for 3 min to remove the surface oxide. It was then rinsed repeatedly with pure water. The five substrates were sonicated in acetone for 5 min to clean and to remove the surface dust and organic impurities, and subsequently immersed in ethanol for 5 min to remove the acetone. The substrates were then dried in a stream of compressed air. Before spin coating, the substrates were fixed on a rotary coater under vacuum. Aqueous NH_4OH (0.25 mL) was added to form a sol solution (3 mL) and the mixture was stirred at 300 r/min for 13 min to obtain a viscous sol. The sol was then dropped onto the surface of the

substrate. It was spun at a rate of 2000 r/min for 30 s. The spin coating was put in a saturated ethanol vapor atmosphere to prevent the rapid evaporation of the solvent within the silica aerogel film. The obtained silica aerogel film was kept in the saturated atmosphere for 10 min to ensure complete curing. It was then immersed in the ethanol solution for 1 d to strengthen the silica skeleton, and subsequently transferred to n-heptane for 1 d to remove residual water, ethanol, and unreacted precursor from the pores. The silica aerogel film was then hydrophobically modified for 2 d in an n-heptane solution with a 40vol% of HMDS. The modifier was renewed twice. Finally, the wet silica aerogel film was dried at room temperature for 24 h under atmospheric pressure.

1.2 Characterization

The interfacial bonding states was observed by ESCALAB™ 250XI X-ray photoelectron spectroscopy (XPS) from Thermo Scientific Instruments by physically peeling the silical aerogel films from the substrates. Spectroscopic ellipsometry measurements were performed to obtain the refractive indices of the coatings over a large spectral range (380–780 nm). The measurements were obtained at room temperature at an incidence angle of 70° with 10 nm in wavelength steps over the spectral range. Each refractive index (n) was fitted from the ellipsometry data with an accuracy of ±0.005 for the wavelength λ =632.8 nm. The AFM measurements were carried out using a Bruker Tensor system. The topographical 2D AFM images were obtained from scales of 5 μm×5 μm and 0.5 μm×0.5 μm. NanoScope Analysis software was used for visualization and subsequent statistical data analysis, including the calculation of the root mean square (RMS) roughness. The water contact angle (CA) values were measured using a JC2000D2 instrument (Shanghai Zhongchen Digital Technology Co., Ltd). A droplet of water was placed on the surface of each substrate. This was repeated three times to obtain the average CA value. The morphologies of the surface and cross-section of each silica aerogel film were investigated by field emission scanning electron microscopy (FESEM, Hitachi Su8220) at 0.5 kV. Cross-sections were prepared using the classical method of breaking by hand without mechanical polishing. The pore distributions of silica aerogel films on various substrates were obtained by Image J software based on the SEM photographs. In order to ensure the accuracy of statistical data, the silica sol was spin-coated on the same type of substrate three times and each sample was photographed five times. Finally 1000 points were selected for each photo and then, they were divided into 10 groups to obtain the frequency.

2 Results and Discussion

2.1 XPS spectra and refractive index of silica aerogel films

The components of the silica aerogel films were characterized by XPS. Fig. 1 shows the X-ray photoelectron spectra of the silica aerogel films. According to Fig. 1a, the silica aerogel films comprises O, Si, N, C, and Na. The Si and O are from the hydrolysis and condensation of TEOS. The N and C are from the HMDS, and transferred to the silica aerogel skeleton by reaction with the hydroxyl groups. Na is introduced from impurities in the glassware, and also connected with the silica through the hydroxyl groups. Fig.1b–1e are high-resolution spectra showing the interfacial bonding state changes of the Al, Ti, SiO_2, and GaN substrates, respectively, during the fabrication of the silica aerogel films.

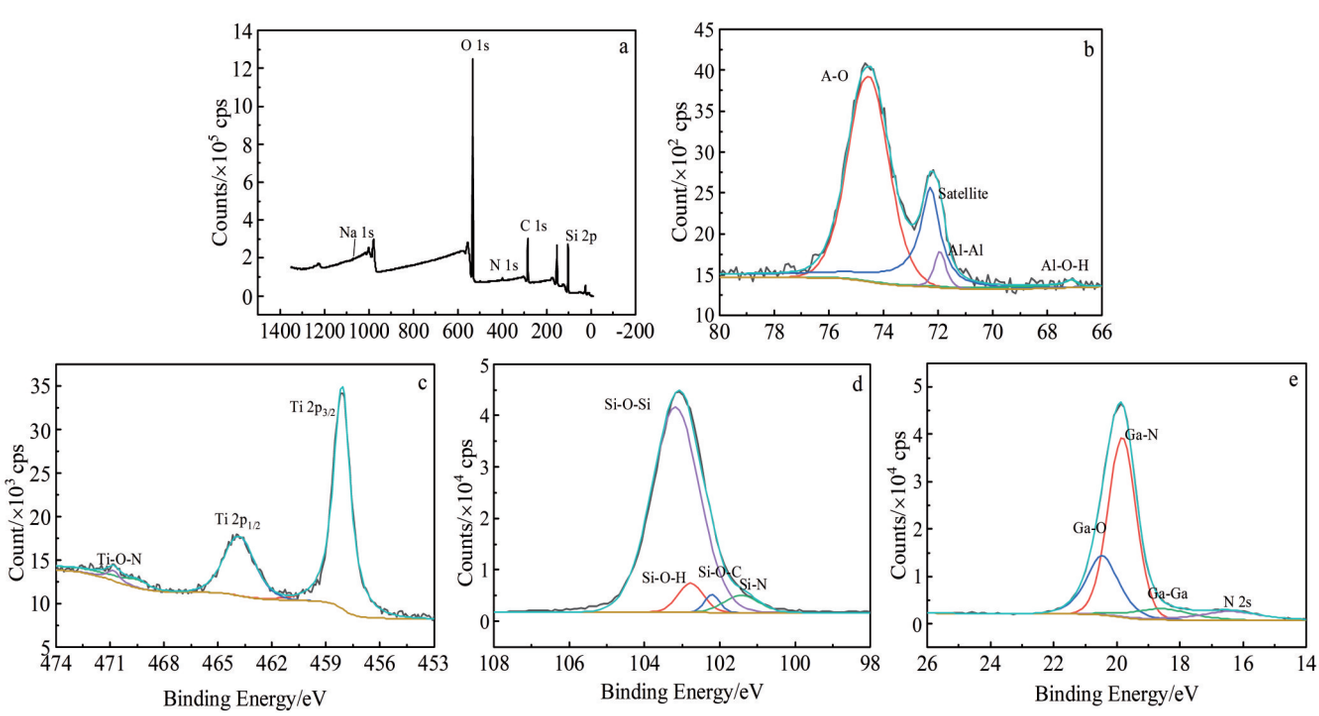

Fig.1 XPS spectra of silica aerogel films (a) and core level spectra of Al 2p (b), Ti 2p (c), Si 2p (d) and GaN (e)

As shown in Fig. 1b, the Al 2p core level spectra feature peak at 74.53 eV is attributable to Al-O bonds and the one at 71.93 eV is attributable to Al-Al bonds. There is a binding energy difference of 0.07 eV between the Al-O peaks and the standard electron binding energy of Al_2O_3 (74.6 eV), which is due to the reaction between Al_2O_3 and -OH. The central peaks at 72.28 eV are the satellite peaks of Al_2O_3. The central peaks at 67.11 eV confirm the presence of aluminum hydroxide. In Fig. 1c, the difference between the central peaks at 458.07 and 463.77 eV is 0.57 eV, which corresponds to the difference between Ti $2p_{3/2}$ and Ti $2p_{1/2}$; therefore, those peaks are assigned to Ti $2p_{3/2}$ and Ti $2p_{1/2}$, respectively, and represent TiO_2. Compared with the standard electron binding energy of TiO_2, the central peak position of Ti $2p_{3/2}$ shifts to a lower binding energy by nearly 0.43 eV, because the formation of Ti-O-H reduces the electron binding energy of the TiO_2. The presence of Ti-O-N bonds is also confirmed by the Ti 1s spectrum. The Si 2p core level spectra are shown in Fig. 1d. The peaks at 103.12 and 102.21 eV are assigned to Si-O-Si bonds and Si-O-C bonds, respectively. The central peak at 101.43 eV represents Si-N bonds, which are formed from the remaining silica aerogel on the SiO_2 substrate. The central peak at 102.78 eV is attributed to Si-O-H bonds, which form during the reaction between the SiO_2 and -OH groups in the silica aerogel film and H_2O in the air. Fig. 1e shows the typical Ga 3d core level spectra. The peaks located at 20.9, 20.3 and 18.5 eV are corresponding to Ga-N, Ga-O and Ga-Ga bonds, respectively. The peak at 16.4 eV is from the overlap N 2s state[40].

In the present study, the gel time was controlled within 20 min by adjusting the amount of ammonia catalyst. After condensation for 13 min, the sol was dripped onto the surface of the substrate and immediately spin-coated. The porous structure of the silica aerogel film was confirmed by measuring its refractive index. The refractive index was determined at various positions, i. e., the center and both edges, as indicated by A – F in Fig. 2b. The indices were measured three times to obtain the average value. The porosity is calculated using the following formula:

$$p = \frac{n_{\text{Silica}} - n_{\text{Aerogel}}}{0.458} \quad (1)$$

where p represents the porosity of the silica aerogel film, and n_{Silica} and n_{Aerogel} represent the refractive indices of solid silica and the silica aerogel, respectively. n_{Silica} has a constant value of 1.458.

The results are shown in Fig. 2a, which reveals that the silica aerogel film has different refractive indices at different positions. Refractive index at the edge is greater than at the center. This can be attributed to the accumulation of particles under centrifugal force at the edge, which leads to an increase in density there. The silica aerogel film on the Ti substrate has a minimum refractive index of approximately 1.17 at the center, corresponding to a porosity of 62.8%. The Al, SiO_2 and GaN substrates have refractive indices of approximately 1.175, 1.183 and 1.185, respectively. The silica aerogel film on the Si substrate has the greatest refractive index (1.196)

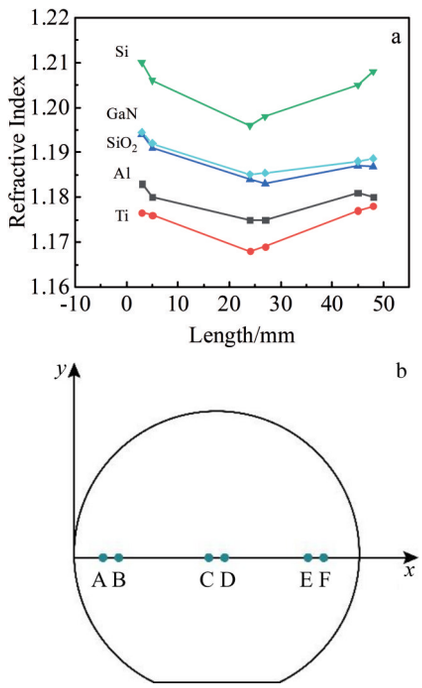

Fig.2 Refractive index of silica aerogel films on five substrates (a) and corresponding positions (b) (left edge: A, B; central region: C, D; right edge: E, F)

and a porosity of approximately 57.2%. The results suggest that the silica aerogel film on the Ti substrate has the lowest density.

2.2 Microstructure of silica aerogel films

The sol was deposited on different substrates at the same spin-coating rate and for the same duration time. It is believed that the fabrication of silica aerogel film is carried out by a chemical hydrolysis-condensation process, also as a result of the nucleation, growth, and aggregation of particles, which will be affected by the substrate type. AFM photographs at different scales are shown in Fig. 3. Fig. 3a – 3e show the surface topographies of the silica aerogel films on Ti, SiO_2, GaN, Al, and Si substrates on scales of 0.5 μm× 0.5 μm. It is clear that the silica aerogel films on the Ti, SiO_2, GaN, and Al substrates contain large particles that are aggregated, whereas the silica aerogel film on the Si substrate has small particles that are less aggregated. The silica aerogel film on the Ti substrate exhibits the strongest accumulation of particles. It also has the largest particles and the largest clusters of particles compared with the films on the other substrates. Some of the particles merge with each other to generate large blocks. In contrast, the silica aerogel film on the Si substrate contains the smallest particles and the smallest clusters. The clusters are uniformly dispersed in the silica aerogel film. Fig. 3f – 3j show the topographies of the silica aerogel films on Ti, SiO_2, GaN, Al, and Si substrates on a scale of 5 μm×5 μm. The roughness of each silica aerogel film on the Si, Al, GaN, SiO_2, and Ti substrates increases in the same order as the particle size and the accumulation of particles on the substrates. In particular, it is clear that the

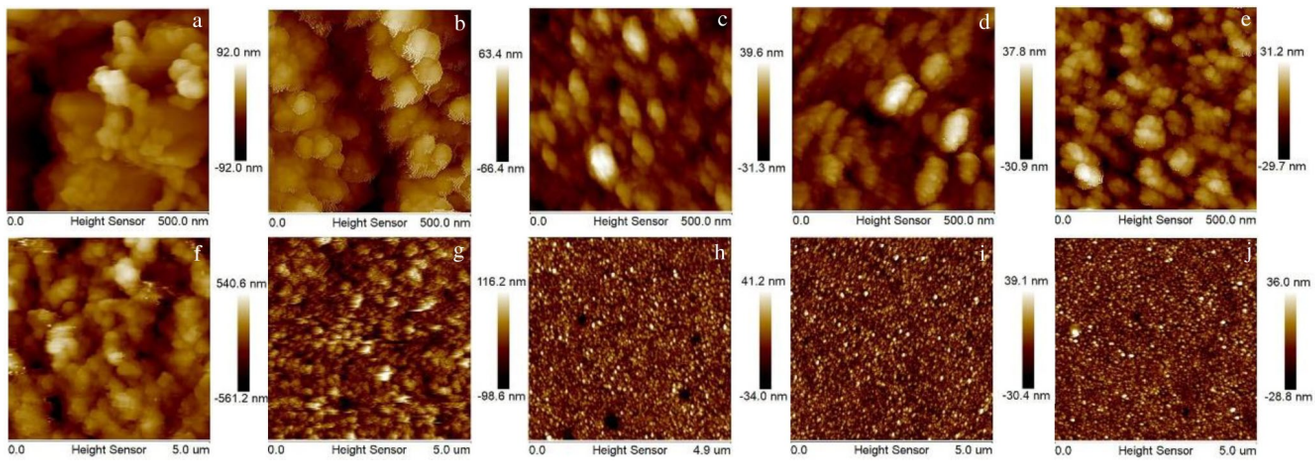

Fig.3 AFM images of silica aerogel films at scales of 0.5 μm×0.5 μm (a–e) and 5 μm×5 μm (f–j) on various substrates: (a, f) Ti, (b, g) SiO_2, (c, h) GaN, (d, i) Al, and (e, j) Si

silica aerogel film on the Ti substrate comprises large aggregations. The reason for this is that the large particles and clusters lead to prolific cross-linking and high viscosity, which impede the dispersion of the solution at the same spin-coating rate used for other coatings.

The effect of the substrate type on the morphology of the silica aerogel film is believed to be associated with the surface hydrophilicity. Therefore, the surface morphologies of the silica aerogel films were investigated by SEM, and the water contact angles on various substrates were also measured. The results are shown in Fig. 4a–4e (the water contact angles on various substrates are shown in the upper right corners of the images). According to the images, the Ti, SiO_2, GaN, Al, and Si substrates have water contact angles of 28.8°, 55.5°, 56.1°, 61.7°, and 74°, respectively, suggesting that the Ti substrate has the highest hydrophilicity; therefore, the SiO_2, GaN, Al, and Si substrates are less hydrophilic. Obviously, the silica aerogel film on the Ti substrate has the most relaxed structure, which consists of large pores and clusters. The silica aerogel films on the Al, GaN and SiO_2 substrates have non-uniform pore distributions and rough skeletons. The silica aerogel film on the Si substrate has small pores and a uniform pore distribution. Fig. 4f shows the statistical pore diameter distributions of silica aerogel films on different substrates, where the average pore diameters are 67.25, 20.69, 20.16, 35.6, and 14.89 nm for the Ti, SiO_2, GaN, Al and Si substrates, respectively.

According to the analysis of the AFM images described above, the difference in the morphologies is a result of particle accumulation. Because the particles are close in the silica aerogel film on the Ti substrate, it is easier for them to attract neighboring particles and molecules through van der Waals forces and electrostatic attractions. Therefore, they form clusters or merge into large particles. This facilitates particle growth. However, on the Si substrate, the greater distances between the particles impede their connection with each other. Moreover, owing to their low mass and surface charge, the small particles are difficult to attract neighboring molecules to merge. The growth of particles becomes difficult, and can only proceed by free diffusion and random collision. Small particles inevitably result in small pores and uniform pore distribution. Considering the water contact angle and the FESEM images, the morphology of each silica aerogel film is related to the hydrophilicity of substrate. It is easier to form large particles and pores on hydrophilic substrates. In general, the hydrophilicity of substrate depends on its molecular polarity: the larger the molecular polarity, the higher the hydrophilicity. Therefore, there is greater potential for the formation of large particles and pores.

Cross-sections of the silica aerogel films were investigated by FESEM. They are displayed in Fig. 5a–5e (the interface is magnified in the upper right corner of each image). There is a close adhesion between the five substrates and the silica aerogel films. In the case of the Si substrate, adhesion is poor and there is an obvious gap between the substrate and the silica aerogel film. This is due to the chemical characteristics of the substrate. Silica aerogel films fabricated by the sol-gel method contain numerous hydroxyl groups on the silica skeleton. When particles grow, hydroxyl groups interact with the polar groups on the surface of hydrophilic substrate, forming hydrogen bonds. Therefore, the adhesion between the substrate and the silica aerogel film is enhanced by the formation of chemical bonds. However, in the case of the HF-treated hydrophobic Si substrate, bond formation by hydroxyl groups is impeded owing to the absence of polar groups. As a result, adhesion between the Si substrate and the silica aerogel film is weak.

2.3 Effect of hydrophilicity on the nucleation

According to the analysis described above, the substrate has a significant effect on the morphology of the silica aerogel film. Hydrophilic surfaces promote large particles and their accumulation, which leads to increased surface roughness, non-uniform pore distribution, and large pores. However, it does promote adhesion between the substrate and the silica aerogel film. In contrast, hydrophobic surfaces produce small highly dispersed particles, smooth surfaces, and small pores.

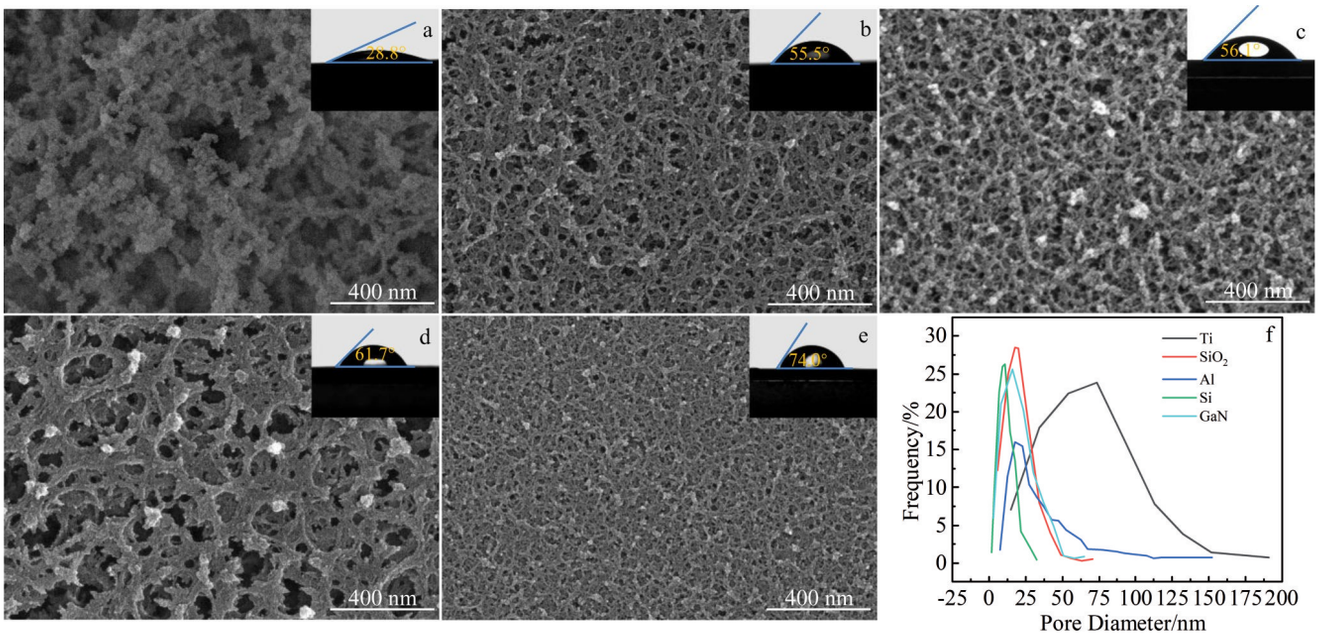

Fig.4 Surface morphologies of silica aerogel films and their corresponding water contact angles on various substrates (a–e) and statistical pore diameter distributions (f): (a) Ti, (b) SiO_2, (c) GaN, (d) Al, and (e) Si

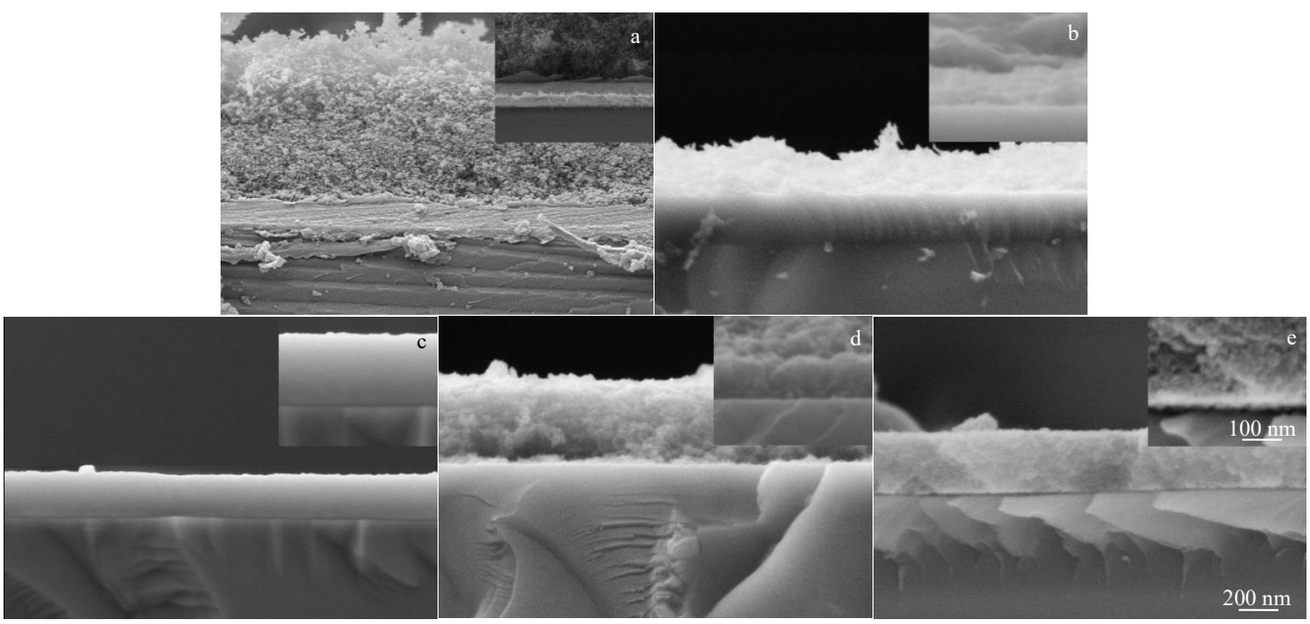

Fig.5 Cross-sections of silica aerogel films on various substrates: (a) Ti, (b) SiO_2, (c) GaN, (d) Al, and (e) Si

However, they also result in poor adhesion between the substrate and the silica aerogel film. The difference is due to the sol-gel fabrication of the silica aerogel film. The gelation process follows the classical nucleation-growth law[41]. During spin coating, the gel molecules aggregate and form tiny particles under the action of surface charges. The tiny particles grow into large ones by interacting with neighboring small molecules through van der Waals's and electrostatic forces[42]. Some of the faster-growing particles become centers of solid nucleation, attracting numerous small particles around the nucleus. Consequently, the particles grow faster by absorbing other particles. Additionally, large particles interact with each other by the physical adsorption and bonding of surface hydroxyl groups to form the clusters that make up a three-dimensional skeleton. However, the substrates change the nucleation and growth of the particles by providing additional nucleation sites. Owing to the low nucleation energy, the particles preferentially accumulate and nucleate on the substrate surface. The change has a significant effect on the growth of particles and the final morphology of the silica aerogel. In addition, nanoparticles themselves may have uneven surface structure and surface charge distribution, or

they may have a certain morphology. These characteristics will affect the subsequent interaction and aggregation of particles, thus affecting the structure of the final product[43].

The current study indicates that different types of substrates cause changes of the morphologies of silica aerogel films. This may be attributed to the influence of the hydrophilicity of the substrates on the nucleation and growth of particles. The hydrophilicity of a substrate depends on its molecular polarity. Hydrophilic substrates are usually composed of polar molecules, which result in positive and negative potentials on the surface. The hydrophilicity of silica substrate is caused by the electrical difference between oxygen and silicon. For Al and Ti substrates, hydrophilicity is caused by the electrical differences between the metal and oxygen atoms, because Al_2O_3 and TiO_2 usually form on the surfaces of the substrates. Owing to the difference in surface potential, the oxygen atoms on the surface bond with the hydroxyl groups of the silica aerogel skeletons to form hydrogen bonds. For GaN substrate, the nitrogen atoms replaces the role of oxygen atoms. Additionally, owing to the similarity in the molecular composition, besides the hydrogen bonds between the silica substrate and the silica aerogel film, weak Si-O bonds between the silica and the hydroxyl groups may also form, which is illustrated in Fig.6a.

According to the classical nucleation theory, the nucleation rate can be expressed as follows[44]:

$$J = K\mathrm{e}^{\left(\frac{-\Delta G_i}{K_B T}\right)} \tag{2}$$

where K represents the dynamic pre-exponential factor, ΔG_i is the Gibbs free energy to form the cluster I, K_B is the Boltzmann constant, and T is temperature. The nucleation barrier is determined by the volume free energy and the surface free energy

$$\Delta G_i = \Delta\mu_i + \sigma A_i \tag{3}$$

where $\Delta\mu_i$ represents the change of chemical potential of the cluster I, σ represents surface free energy, and A_i represents surface area of the cluster i. The formation of molecular bonds reduces the interfacial energy between the nucleus and the substrate, resulting in the decrease of ΔG_i and the increase of J. Because the wetting angle decreases with the interfacial energy, the interface energy can be expressed in terms of the wetting angle. The effect of the wetting angle on nucleation energy follows the classical nucleation theory:

$$\Delta G_{het} = \Delta G_{homo} f(\theta) \tag{4}$$

$$f(\theta) = 0.25(2 - 3\cos\theta + \cos^3\theta) \tag{5}$$

where ΔG_{homo} and ΔG_{het} represent the Gibbs free energy for homogeneous and heterogeneous nucleation, respectively; θ is the wetting angle. When $\theta < 90°$, the substrate will reduce nucleation energy and improve the efficiency of nucleation significantly. The large nucleation rate and low nucleation energy lead to the massive accumulation of particles on the surface of the hydrophilic substrate, which shortens the distance between particles and produces many nucleation sites. Neighboring particles merge with each other to form large ones. The large particles and clusters become the new nucleation sites[45], which create new larger particles, speeding up the whole gel process. In summary, the hydrophilicity of the substrate accelerates nucleation and growth, leading to the formation of large particles. On the contrary, there is no significant surface potential difference for hydrophobic substrates. The accumulation of particles on the surface of the substrate is reduced. The nucleation and growth of gel particles occur through the random collision and bonding of gel molecules. Particles grow through absorbing neighboring small molecules and particles under the action of van der Waals's and electrostatic forces, which impede the growth of the particles. However, the slow growth results in smaller particles and a more uniform morphology compared with the particles and morphology of a hydrophilic substrate. Effect of the substrate types on the morphology of silica aerogel film is shown in Fig.6b.

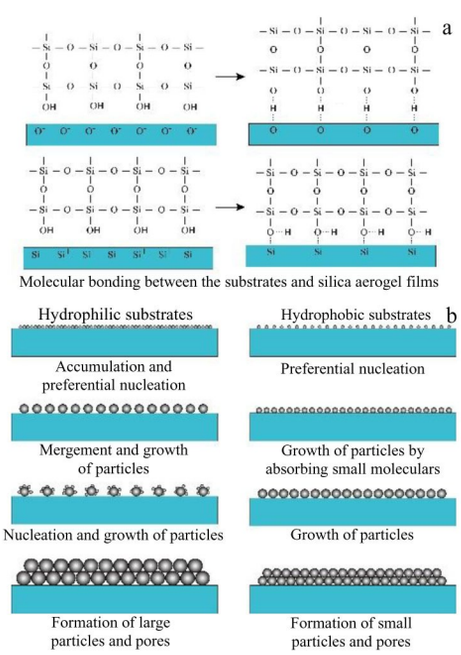

Fig.6 Fabrication of silica aerogel films on substrates: (a) molecular bonds at the interface between the hydrophilic substrate and the silica aerogel film; (b) accumulation and growth of particles on hydrophilic (left) and hydrophobic (right) substrates

3 Conclusions

1) Chemical bonds between substrates of Al and Ti and the silica aerogel films are confirmed by XPS measurement. Meanwhile, the silica aerogel film on the Ti substrate has a minimum refractive index of approximately 1.17 at the center, and the porosity is up to 62.8%.

2) Ti substrate with the highest hydrophilicity causes the greatest accumulation of particles in the silica aerogel film, which results in large particles, large pores, and high roughness. The hydrophilicity is weaked in an order of SiO_2, GaN, Al and Si substrates. The silica aerogel film on Si substrate with weak hydrophilicity has the smallest particles

and pores and small roughness.

3) Nucleation is easier in a silica aerogel film on a hydrophilic substrate; the particles aggregate more readily and grow to form large particles, leading to the formation of larger pores. Owing to weak molecular polarity, the accumulation of particles on the surface of hydrophobic substrate is reduced, and the nucleation and growth of particles are impeded.

References

1 Lamy-Mendes A, Pontinha A D R, Alves P *et al. Construction and Building Materials*[J], 2021, 286(2): 122 815

2 Liu Y C, Wu H J, Zhang Y H *et al. Energy and Buildings*[J], 2020, 228: 110 452

3 Wang W Q, Zhang Z H, Zu G Q. *Rare Metal Materials and Engineering*[J], 2016, 45(S1): 421

4 Wicikowska B, Nowak A P, Trzciński K *et al. Procedia Engineering*[J], 2014, 98: 42

5 Feng J D, Le D Y, Nguyen S T *et al. Colloids and Surfaces A-Physicochemical and Engineering Aspects*[J], 2016, 506: 298

6 Wang J C, Shen J, Ni X Y *et al. Rare Metal Materials and Engineering*[J], 2010, 39(S2): 14

7 Kumar G, Dora D, Jadav D *et al. Journal of Cleaner Production*[J], 2021, 298: 126 744

8 Tang R H, Hong W, Srinivasakannan C *et al. Separation and Purification Technology*[J], 2021, 281: 119 950

9 Liu Q, Liu Y, Zhang Z H *et al. Chinese Journal of Chemical Engineering*[J], 2020, 28(9): 2467

10 Al-Soubaih R M, Saoud K M, Ye F *et al. Microporous and Mesoporous Materials*[J], 2020, 292: 109 758

11 Orlovi A, Janakovi D, Skala D. *Catalysis Communications*[J], 2002, 3(3): 119

12 Zhao S, Bo J, Maeder T *et al. ACS Applied Materials & Interfaces*[J], 2015, 7(33): 18 803

13 Peng F, Jiang Y G, Feng J *et al. Chemical Engineering Journal*[J], 2021, 411: 128 402

14 Shi C X, Zhang S C, Jiang Y G *et al. Rare Metal Materials and Engineering*[J], 2016, 45(S1): 210

15 Anyfantakis M, Baigl D, Binks B P *et al. Langmuir: The ACS Journal of Surfaces and Colloids*[J], 2017, 33: 5025

16 Wang W D, Grozea D, Kim A *et al. Advanced Materials*[J], 2010, 22(1): 99

17 Pan F M, Wu B W, Cho A T *et al. Journal of Vacuum Science & Technology*[J], 2004, 22(3): 1067

18 Yin Y J, Wang C X, Wu M *et al. Journal of Materials Science*[J], 2011, 46(20): 6682

19 Le H N T, Jeong H K. *Chemical Physics Letters*[J], 2014, 592: 349

20 Uzum A, Fukatsu K, Kanda H *et al. Nanoscale Research Letters* [J], 2014, 9(1): 659

21 Faraco T A, Yoshioka N A, Sábio R M *et al. Nanotechnology*[J], 2021, 32(20): 205 603

22 Kowada Y, Ozeki T, Minami T. *Journal of Sol-Gel Science and Technology*[J], 2005, 33(2): 175

23 Wang G J, Yang J Y, Shi Q. *Journal of Coatings Technology & Research*[J], 2011, 8(1): 53

24 Zhang T T, Huang J, Zhang R Z *et al. Advanced Materials Research*[J], 2013, 756–759: 150

25 Hao Y, Pi P H, Cai Z Q *et al. Applied Surface Science*[J], 2010, 256(13): 4095

26 Yavas H, Seluk C D O, Sinan Özhan A E *et al. Thin Solid Films*[J], 2014, 556(4): 112

27 Thompson W R, Pemberton J E. *Analytical Chemistry*[J], 1994, 66(20): 3362

28 Thompson W R, Pemberton J E. *Langmuir*[J], 1995, 11(5): 1720

29 Alford T L, Chen L H, Gadre K S. *Thin Solid Films*[J], 2003, 429(1–2): 248

30 Li Y, Gao D, Guo Y F *et al. Chemical Engineering Journal*[J], 2022, 427: 131 746

31 Thompson W R, Pemberton J E. *Chemistry of Materials*[J], 1995, 7(1): 130

32 Rai A, Perry C C. *Journal of Materials Chemistry*[J], 2012, 22(11): 4790

33 Xu Lin, Ding J N, Xu X J *et al. Rare Metal Materials and Engineering*[J], 2017, 46(1): 127 (in Chinese)

34 Fu W B, Liu J H, Liang J H *et al. Rare Metal Materials and Engineering*[J], 2016, 45(3): 623 (in Chinese)

35 Nie X L, Ma D Y, Ma F *et al. Rare Metal Materials and Engineering*[J], 2018, 47(1): 64

36 Predoana L, Nicolescu M, Preda S *et al. Journal of Sol-Gel Science and Technology*[J], 2014, 71(2): 303

37 Sun X Y, Wu C G, Luo W B *et al. Rare Metals*[J], 2019(1): 1

38 Jung S B , Park H H, Kim H. *Thin Solid Films*[J], 2004, 447–448: 575

39 He C G, Zhao W, Wu H L *et al. ACS Applied Materials & Interfaces*[J], 2017, 9(49): 43 386

40 Grodzicki M, Rousset J G, Ciechanowicz *et al. Vacuum*[J], 2019, 167: 73

41 Servi I S, Turnbull D. *Acta Metallurgica*[J], 1966, 14(2): 161

42 Hong X T, Willing G A. *Review of Scientific Instruments*[J], 2008, 79(12): 930

43 JJ De Yoreo, Gilbert P U, Sommerdijk N A *et al. Science*[J], 2015: 349

44 Cölfen H, Antonietti M. *Colloidal Crystals with Spherical Units: Opals and Colloidal Nanocrystals*[M]. New Jersey: John Wiley& Sons, Ltd, 2008: 107

45 Watzky M A, Finke R G. *Journal of the American Chemical Society*[J], 1997, 119(43): 10 382

常压干燥法制备过程中衬底类型对二氧化硅气凝胶薄膜形貌的影响

郑　伟[1]，王　垚[1]，何思亮[2]，向　讯[1]，崔银花[1]，胡　川[1]

(1. 广东省科学院半导体研究所，广东 广州 510650)

(2. 桂林电子科技大学 机电工程学院，广西 桂林 541004)

摘　要：采用常压干燥法，在Ti、SiO_2、GaN、Al和Si 5种衬底上制备二氧化硅气凝胶薄膜，研究衬底类型对二氧化硅气凝胶薄膜形貌的影响。通过XPS法检测二氧化硅气凝胶薄膜与衬底之间的界面结合。采用椭偏仪结合反射光谱拟合的方法对二氧化硅气凝胶薄膜的折射率进行测量。通过原子力显微镜和场发射扫描电镜对二氧化硅气凝胶薄膜的表面及截面形貌进行观测。结果表明，二氧化硅气凝胶薄膜的形成会导致Al衬底表面Al-O中心峰产生0.07 eV的偏离，以及Ti衬底表面Ti $2p_{3/2}$中心峰0.43 eV的偏离。这表明Al衬底和Ti衬底与二氧化硅气凝胶薄膜之间形成了某种化学键。同时，折射指数测量显示，Ti衬底表面形成的二氧化硅气凝胶薄膜折射指数最低（1.17），平均孔隙率（63.8%）比硅衬底表面形成的二氧化硅气凝胶薄膜孔隙率（57.2%）要高。衬底类型对二氧化硅气凝胶薄膜形貌的影响与不同衬底的亲水性有关。由于Ti衬底亲水性最佳，更多的颗粒在Ti衬底表面形核和长大，导致其上制备的二氧化硅气凝胶薄膜具有更大的表面粗糙度，以及更大的颗粒和孔径。

关键词：二氧化硅气凝胶薄膜；衬底类型；亲水性；分子极性；颗粒形核与长大

作者简介：郑　伟，男，1988年生，博士，广东省科学院半导体研究所，广东 广州 510650，E-mail：1210557964@qq.com